

# Superlinear and sublinear urban scaling in geographical network model of the city

K. Yakubo\* and Y. Saijo

*Department of Applied Physics, Hokkaido University, Sapporo 060-8628, Japan*

D. Korošak†

*University of Maribor, Slomškov trg 15, Maribor SI-2000, Slovenia*

(Dated: February 27, 2022)

Using a geographical scale-free network to describe relations between people in a city, we explain both superlinear and sublinear allometric scaling of urban indicators that quantify activities or performances of the city. The urban indicator  $Y(N)$  of a city with the population size  $N$  is analytically calculated by summing up all individual activities produced by person-to-person relationships. Our results show that the urban indicator scales superlinearly with the population, namely,  $Y(N) \propto N^\beta$  with  $\beta > 1$  if  $Y(N)$  represents a creative productivity and the indicator scales sublinearly ( $\beta < 1$ ) if  $Y(N)$  is related to the degree of infrastructure development. These coincide with allometric scaling observed in real-world urban indicators. We also show how the scaling exponent  $\beta$  depends on the strength of the geographical constraint in the network formation.

**PACS numbers:** 89.75.Da, 89.65.Lm, 89.65.-s, 89.75.Hc

## I. INTRODUCTION

Cities are often compared to living organisms with a hierarchical organization consisting of cells, tissues and organs. Likewise, people in a city form groups, groups form organizations serving certain functions, and interdependent complex relationships between functional organizations sustain the whole urban activities. Such similarities are not only found in the correspondence between constituent elements of cities and living organisms but also in allometric scaling. As is a metabolic rate of a complex organism proportional to the  $3/4$  power of body mass [1, 2], various quantities related to activities or performances of a city depend on the scale of the city in a power-law manner [3–12]. In particular, extensive work [13–29] has revealed that an urban indicator  $Y$  quantifying city activity scales, on average, with the population size  $N$  as a power-law:

$$Y(N) \propto N^\beta, \quad (1)$$

where  $\beta$  is a scaling exponent. Bettencourt *et al.* [15–17] have found that an urban indicator representing a creative productivity, such as: the number of new patents, the gross domestic product (GDP), the number of crimes, etc., obeys a superlinear scaling law ( $\beta > 1$ ) while an indicator related to the degree of infrastructure development, such as the total length of electrical cables, the number of gas stations, the total road surface, etc., scales sublinearly with the population size ( $\beta < 1$ ). Due to the nonlinear scaling Eq. (1), a meaningful comparison between characteristics of individual cities requires evaluations of deviations from this average scaling behavior, instead of considering per capita quantity  $Y(N)/N$  [18–21].

It is crucial to understand the reason why urban indicators representing creative productivities scale superlinearly and those corresponding to material infrastructures scale sublinearly. Arbesman, Kleinberg, and Strogatz [30] have proposed a network model (AKS model) to explain superlinear scaling found in creative productivities. They introduced hierarchical social distances between nodes representing people in a city. A network is formed by connecting nodes with the edge probability decaying exponentially with the social distance. Assuming that the individual productivity yielded by an edge increases exponentially with the social distance, the AKS model gives superlinear scaling of creative productivity  $Y(N)$  if the total contribution from connected node pairs separated by the social distance  $d$  is an increasing function of  $d$ , giving linear scaling otherwise.

In order to explain both superlinear and sublinear scaling of urban indicators, Bettencourt [31] has worked with four simple assumptions: (1) Citizens explore the city fully to benefit from it and the city develops in a way to make this possible. (2) The infrastructure network volume  $A_n$  grows in a decentralized way in order to connect each addition of a new inhabitant, namely,  $A_n \propto Nr$ , where  $N$  is the number of people in the city and  $r$  is the average distance between individuals. (3) The product of average social output and the volume spanned by individual's movement is constant of city size  $N$ , which means that human effort is bounded. (4) The urban indicator  $Y(N)$  related to a creative productivity is proportional to the number of local social interactions. According to the Bettencourt's model, the scaling exponent is given by  $\beta = 1 + \delta$  for the superlinearly scaled creative productivity and  $\beta = 1 - \delta$  for the sublinearly scaled infrastructure volume, where  $\delta$  is a positive exponent that depends on the fractal dimension of human travel paths.

Despite these two pioneering and suggestive theories, the mechanism of urban scaling has not yet been completely understood. Although the AKS model [30] gives

\* yakubo@eng.hokudai.ac.jp

† dean.korosak@um.si

a possible explanation of superlinear (or linear) scaling of creative productivities and describes how the social structure (i.e., human relations) affects the scaling exponent  $\beta$ , sublinear scaling for urban indicators reflecting infrastructures has not been argued. On the other hand, the Bettencourt's model [31] demonstrates both superlinear and sublinear scaling for a creative productivity and an infrastructure volume, respectively. However, it is not clear how the social structure influences urban scaling, because this theory is based on a continuum model. Furthermore, the scaling exponent  $\beta$  always appears symmetrically as  $\beta = 1 \pm \delta$  for superlinear and sublinear scaling, hence a variety of real-world nonlinear urban scaling cannot be described by this model. It is therefore important to explain consistently both superlinear and sublinear scaling in the context of the relation between the scaling behavior and the social structure in the city.

In this paper, we propose a model to account for urban scaling by representing human relations in a city by a geographical network in which nodes close to each other are more likely to be connected. It is assumed that an urban indicator  $Y(N)$  is given by the sum of the activities produced by individual connected node-pairs and that the individual activity  $y_{ij}$  depends on the Euclidean distance  $l_{ij}$  between connected nodes  $i$  and  $j$ . We show that the urban indicator scales superlinearly or linearly with the population size  $N$  when the activity  $y_{ij}$  represents a creative productivity that is an increasing function of the Euclidean distance  $l_{ij}$  and scales sublinearly or linearly if  $y_{ij}$  decreases with  $l_{ij}$  as the strength of the demand for infrastructure does. This result is consistent with observed urban scaling phenomena. We also predict that urban indicators representing either creative productivities or infrastructures are proportional to the population size (i.e., linear scaling) if the geographical constraint in the network formation is strong enough.

The paper is organized as follows. After presenting our model in Sec. II, the urban scaling exponent  $\beta$  is analytically calculated in Sec. III. Numerical confirmations for analytical results are given in Sec. IV. We also show here how the exponent  $\beta$  depends on parameters characterizing our model. Finally, we conclude our work in Sec. V.

## II. THE MODEL

### A. Geographical network model

It has been demonstrated that urban structure possesses a self-similar property, i.e., the fractal nature of population density in a city [4, 32–35]. In our model,  $N$  nodes representing people in a city are located homogeneously in a fractal space  $S_D$  with the fractal dimension  $D$ . The Euclidean distance is defined for any pair of nodes. The fractal space  $S_D$  with the linear size  $L$  is assumed to be large enough and isotropic from any point

in  $S_D$ . Thus, the number of nodes or the population size of the city is presented by

$$N = \rho L^D, \quad (2)$$

where  $\rho$  is a coefficient. Each node (person) has its own ability or charm to attract others. In order to quantify such personal attractiveness, a real continuous quantity  $x$  (referred as ‘attractiveness’ hereafter) is randomly assigned for each node according to the power-law probability distribution function  $s(x)$  expressed by

$$s(x) = s_0 x^{-\alpha}, \quad (x \geq x_{\min}), \quad (3)$$

where  $\alpha > 1$ ,  $x_{\min} > 0$ , and the normalization constant  $s_0$  is given by

$$s_0 = (\alpha - 1) x_{\min}^{\alpha-1}. \quad (4)$$

Since it is natural to consider that two nodes spatially close to each other and having large attractiveness values are more likely to be connected, two nodes  $i$  and  $j$  are connected if the following condition is satisfied,

$$\frac{x_i x_j}{l_{ij}^m} > \Theta, \quad (5)$$

where  $l_{ij}$  denotes the Euclidean distance between the nodes  $i$  and  $j$ ,  $m (\geq 0)$  is a parameter controlling the strength of the geographical constraint in the network formation,  $x_i$  is the attractiveness of the node  $i$ , and  $\Theta$  is a threshold value.

Statistical properties of networks formed by the above procedures have been studied previously [36, 37]. We briefly summarize the results of these works here. First, the network exhibits the scale-free property, that is, the distribution  $P(k)$  of the degree  $k$  follows a power law,

$$P(k) \propto k^{-\gamma}, \quad (6)$$

for large  $k$  [36, 37]. The exponent  $\gamma$  is related to the model parameters  $D$ ,  $\alpha$ , and  $m$  through [37]

$$\gamma = \begin{cases} 2 & \text{if } D \geq d_c, \\ 1 + \frac{d_c}{D} & \text{if } D < d_c, \end{cases} \quad (7)$$

where

$$d_c = m(\alpha - 1). \quad (8)$$

This result shows that the degree distribution becomes more homogeneous when the geographical constraint is enhanced by increasing  $m$ . This is because the network formed by a large  $m$  value has a lattice-like structure.

Second, the probability distribution function  $R(l)$  of the edge length  $l$  is proportional to the average number of edges,  $k(l)dl$ , of the length in the range of  $[l, l + dl]$  from a given node. These are given by [37]

$$R(l) \propto k(l) \propto \begin{cases} l^{D-1} & \text{if } l \leq \xi, \\ l^{D-1} \left(\frac{l}{\xi}\right)^{-d_c} & \text{if } l > \xi, \end{cases} \quad (9)$$

where

$$\xi = \left( \frac{x_{\min}^2}{\Theta} \right)^{1/m}. \quad (10)$$

The quantity  $\xi$  is the distance below which any two nodes are connected regardless of the attractiveness  $x$ . Here, we neglected a logarithmic correction term. The probability of two nodes separated by the Euclidean distance  $l$  to be connected by an edge is directly obtained from Eq. (9). This probability  $g(l)$  is presented by the ratio of  $k(l)dl$  to the number of nodes  $n(l)dl$  located at a distance within the range of  $[l, l + dl]$  from a given node. Since  $n(l) \propto l^{D-1}$ , the relation  $g(l) = k(l)/n(l)$  immediately leads

$$g(l) = \begin{cases} 1 & \text{if } l \leq \xi, \\ \left( \frac{l}{\xi} \right)^{-d_c} & \text{if } l > \xi. \end{cases} \quad (11)$$

The power-law decay of  $g(l)$  for  $l > \xi$  is consistent with the fact that the probability of two persons separated by  $l$  to be socially connected decreases with  $l$  in a power-law manner [38–41]. The relation  $g(l) = 1$  for  $l \leq \xi$  is obvious from the meaning of the distance  $\xi$ .

Third, the average degree  $\langle k \rangle$  of the network can be controlled by tuning the threshold  $\Theta$ . Although the  $\Theta$  dependence of  $\langle k \rangle$  has been already studied [37], here we clarify not only the  $\Theta$  dependence but the  $N$  dependence of  $\langle k \rangle$ . The average degree is obviously given by

$$\langle k \rangle = \int_0^L k(l) dl, \quad (12)$$

where the linear size  $L$  of the city is related to the population size  $N$  through Eq. (2). Substituting Eq. (9) into Eq. (12),  $\langle k \rangle$  can be calculated as

$$\begin{aligned} \langle k \rangle &= c_1 \int_0^\xi l^{D-1} dl + c_2 \int_\xi^L \left( \frac{l}{\xi} \right)^{-d_c} l^{D-1} dl \\ &= \left( \frac{c_1}{D} - \frac{c_2}{D-d_c} \right) \xi^D + \frac{c_2}{D-d_c} \xi^{d_c} L^{D-d_c}, \end{aligned} \quad (13)$$

where  $c_1$  and  $c_2$  are irrelevant numerical coefficients. Here, we define a new relation symbol “ $\propto$ ” to represent the relation  $A = cx + c'y$  by  $A \propto x + y$  if  $c$  and  $c'$  are nonzero constants independent of  $x$  and  $y$ . Using this notation, Eq. (13) can be written as  $\langle k \rangle \propto \xi^D + \xi^{d_c} L^{D-d_c}$ . Thus, the relation  $L \propto N^{1/D}$  from Eq. (2) and Eq. (10) lead

$$\langle k \rangle \propto \Theta^{-D/m} + \Theta^{-d_c/m} N^{1-d_c/D}. \quad (14)$$

Therefore, we obtain

$$\langle k \rangle \propto \begin{cases} \Theta^{-D/m} & \text{if } D \leq d_c, \\ \Theta^{-d_c/m} N^{1-d_c/D} & \text{if } D > d_c, \end{cases} \quad (15)$$

for a large enough value of  $N$ . These analytical results have been numerically confirmed for uniform node sets in which nodes are uniformly distributed in a two-dimensional space and for fractal node sets in which nodes are placed in a fractal manner [37].

## B. Urban indicator

In order to clarify the scaling property of an urban indicator  $Y(N)$  quantifying activities in a city, we must relate  $Y(N)$  to human relations in the city modeled by a geographical network described above. Although actual urban performances are sometimes produced by a cooperation between many people in a group or an organization, we consider here that the total urban performance stems from one-to-one human relationships, namely from individual connected node pairs in the network. Furthermore, we neglect nonlinear effects such as interactions between individual node-pair activities creating additional activities. These simplifications allows us to write the urban indicator as

$$Y(N) = \frac{1}{2} \sum_{i,j}^N a_{ij} y_{ij}, \quad (16)$$

where  $a_{ij}$  is the  $(i, j)$  element of the adjacency matrix of the network and  $y_{ij}$  is the individual activity between nodes  $i$  and  $j$ .

As in the case of the AKS model [30] in which the individual productivity is assumed to increase with the *social* distance  $d$ , it is natural to consider that the individual activity  $y_{ij}$  depends on the *Euclidean* distance  $l_{ij}$  between nodes  $i$  and  $j$ . Instead of the exponential  $d$ -dependence in the AKS model, we assume a power-law dependence of  $y_{ij}$  on  $l_{ij}$ , i.e.,

$$y_{ij} \propto l_{ij}^\eta, \quad (17)$$

where the exponent  $\eta$  can take either positive or negative values. If  $\eta$  is positive, longer-distance connections give higher individual activities. In this case, we can regard  $y_{ij}$  as an individual creative productivity, because distant individuals have usually different experiences and their values, and the fusion of heterogeneous ideas often leads to greater creativity compared to combinations of homogeneous ideas. This interpretation is consistent with the geographical network model presented in the previous subsection. In the network model, a long-distance connection is established only when two nodes have large attractiveness, namely, they are highly capable. Outputs by collaboration between such talented individuals must be innovative.

On the other hand, if  $\eta$  is negative and  $y_{ij}$  decreases with  $l_{ij}$ , short-distance connections contribute more significantly to the total urban indicator  $Y(N)$  than long-distance ones. In this case, the following consideration suggests that  $Y(N)$  represents an infrastructure volume. The degree of infrastructure development depends on how strong the demand for the infrastructure is. Since infrastructure facility, such as electrical power cables, railway stations, or green open urban spaces, provides services for inhabitants near the facility, the social need for the infrastructure arises from local consensus among neighboring residents in areas having no access to the infrastructure. Thus, the consensus between residents close

to each other must be stronger than that between distant ones. If we regard  $y_{ij}$  given by Eq. (17) with negative  $\eta$  as the strength of the consensus between nodes  $i$  and  $j$ ,  $Y(N)$  provided by Eq. (16) quantifies the whole social need in the city. Considering that infrastructure facilities are realized in proportion to the social need,  $Y(N)$  is proportional to the infrastructure volume.

### III. URBAN SCALING

In this work, we concentrate on the urban indicator averaged over all possible cities with the same population size  $N$  but different spatial arrangements of people. Then, we treat the quantity,

$$Y(N) = \frac{1}{2} \left\langle \sum_{i,j}^N a_{ij} y_{ij} \right\rangle, \quad (18)$$

where  $\langle \dots \rangle$  denotes the average over network configurations with the same parameters  $D$ ,  $\alpha$ ,  $m$ , and  $\eta$ . Using the node connection probability  $g(l)$  by an edge of the length  $l$ , the average urban indicator is presented by

$$Y(N) \propto N \int_0^L g(l) y(l) n(l) dl, \quad (19)$$

where  $n(l)dl$  is the number of nodes within the range of  $[l, l + dl]$  from a given node and  $y(l)$  is the individual activity between nodes separated each other by the distance  $l$ . In this section, we examine the scaling behavior of  $Y(N)$  by evaluating Eq. (19).

Substituting the relations  $y(l) \propto l^\eta$  from Eq. (17),  $n(l) \propto l^{D-1}$ , and Eq. (11) into Eq. (19), we have

$$\begin{aligned} \frac{Y(N)}{N} &\propto: \int_0^\xi l^\eta l^{D-1} dl + \int_\xi^L \left( \frac{l}{\xi} \right)^{-d_c} l^\eta l^{D-1} dl \\ &\propto: \xi^{D+\eta} + L^{D+\eta} \left( \frac{L}{\xi} \right)^{-d_c}, \end{aligned} \quad (20)$$

where the symbol  $\propto:$  has been defined below Eq. (13). Here we assumed

$$\eta > -D, \quad (21)$$

for the convergence of the integral at  $l = 0$ . This condition is, however, not important because of the existence of the minimum node-pair distance in actual spatial arrangements of people. Since the linear size  $L$  is related to  $N$  through Eq. (2),  $Y(N)$  is written as

$$\frac{Y(N)}{N} \propto: \Theta^{-(D+\eta)/m} + \Theta^{-d_c/m} N^{1-(d_c-\eta)/D}, \quad (22)$$

where the characteristic length  $\xi$  in Eq. (20) was replaced with the threshold  $\Theta$  by using Eq. (10). Equation (22)

tells us how the urban indicator scales with the population size  $N$  under a fixed value of the threshold  $\Theta$ .

We should note that as predicted by Eq. (15) the average degree  $\langle k \rangle$  of the network changes as  $N$  increases under a fixed  $\Theta$ . In actual cities, however, the average number of acquaintances corresponding to  $\langle k \rangle$  is almost independent of  $N$ . Therefore, we must reveal the scaling behavior of  $Y(N)$  under a fixed value of  $\langle k \rangle$  instead of a fixed  $\Theta$ . In order to express  $Y(N)$  as a function of  $N$  and  $\langle k \rangle$ , we rewrite Eq. (15) as

$$\Theta \propto \begin{cases} \langle k \rangle^{-m/D} & \text{if } D \leq d_c, \\ \langle k \rangle^{-m/d_c} N^{m(D-d_c)/Dd_c} & \text{if } D > d_c. \end{cases} \quad (23a)$$

In the case of  $D \leq d_c$ , substitution of Eq. (23a) into Eq. (22) yields

$$Y(N) \propto: \langle k \rangle^{1+\eta/D} N + \langle k \rangle^{d_c/D} N^{2+(\eta-d_c)/D}. \quad (24)$$

This relation is valid for a large enough population size, because Eq. (23) derived from Eq. (15) holds for a large  $N$ . In this case, one of two terms in Eq. (24) dominates  $Y(N)$  depending on the value of the exponent of  $N$ . If  $2 + (\eta - d_c)/D \leq 1$ , namely  $D \leq d_c - \eta$ , the first term grows with  $N$  faster than the second term, and we have linear scaling of  $Y(N)$ , i.e.,

$$Y(N) \propto N, \quad \text{if } D \leq d_c \text{ and } D \leq d_c - \eta. \quad (25)$$

For  $D > d_c - \eta$ , however, the second term of Eq. (24) dominates  $Y(N)$ . Thus,  $Y(N)$  scales as

$$Y(N) \propto N^{2+(\eta-d_c)/D}, \quad \text{if } d_c - \eta < D \leq d_c. \quad (26)$$

On the other hand, for  $D > d_c$ , substitution of Eq. (23b) into Eq. (22) leads to

$$\begin{aligned} Y(N) &\propto: \langle k \rangle^{(D+\eta)/d_c} N^{[d_c(2D+\eta)-D(D+\eta)]/Dd_c} \\ &\quad + \langle k \rangle N^{1+\eta/D}. \end{aligned} \quad (27)$$

Similarly to the case of Eq. (24), the comparison between the exponents  $[d_c(2D+\eta)-D(D+\eta)]/Dd_c$  and  $1+\eta/D$  gives

$$Y(N) \propto N^{[d_c(2D+\eta)-D(D+\eta)]/Dd_c}, \quad \text{if } d_c < D \leq d_c - \eta, \quad (28)$$

and

$$Y(N) \propto N^{1+\eta/D}, \quad \text{if } D > d_c \text{ and } D > d_c - \eta. \quad (29)$$

These relations provide nonlinear scaling of the urban indicator  $Y(N)$ .

Summarizing the above results, the scaling exponent  $\beta$  in Eq. (1) is given by

$$\beta = \begin{cases} 1 & \text{if } D \leq d_c \text{ and } D \leq d_c - \eta \\ 2 + \frac{\eta - d_c}{D} & \text{if } d_c - \eta < D \leq d_c \\ 2 + \frac{\eta}{D} - \frac{D + \eta}{d_c} & \text{if } d_c < D \leq d_c - \eta \\ 1 + \frac{\eta}{D} & \text{if } D > d_c \text{ and } D > d_c - \eta \end{cases}$$

(30a)  
 (30b)  
 (30c)  
 (30d)

The exponent  $\beta$  can take any positive value by controlling the four parameters  $D$ ,  $\alpha$ ,  $m$ , and  $\eta$ . This implies that the urban indicator in our model scales superlinearly ( $\beta > 1$ ), linearly ( $\beta = 1$ ), or sublinearly ( $\beta < 1$ ) with the population size  $N$ . Let us consider the value of  $\beta$  by examining each expression of Eq. (30). The exponent  $\beta$  presented by Eq. (30a) obviously leads to linear scaling of  $Y(N)$ . In this case, the exponent  $\eta$  can be positive or negative. If  $\eta \geq 0$ , the condition for Eq. (30a) is read as  $D \leq d_c - \eta$ , namely,  $D + \eta \leq m(\alpha - 1)$ , while it becomes  $D \leq d_c$  [i.e.,  $D \leq m(\alpha - 1)$ ] for  $\eta < 0$ . Next,  $\beta$  by Eq. (30b) is always larger than 1, because  $(\eta - d_c)/D$  is larger than  $-1$  from the condition  $d_c - \eta < D$ . We should note that the condition for Eq. (30b) requires  $\eta > 0$ . On the contrary, Eq. (30c) is the case only when  $\eta < 0$ . Taking into account Eq. (21),  $\eta$  in Eq. (30c) must satisfy  $-D < \eta < 0$  actually. Since  $(D + \eta)/d_c \leq 1$  for Eq. (30c), we have  $\beta \geq 1 + \eta/D$ . In addition, the condition  $\eta > -D$  gives  $\beta > 0$ . Furthermore,  $\beta$  given by Eq. (30c) is expressed as  $\beta = 1 + (D + \eta)(1/D - 1/d_c)$ . Since  $D + \eta > 0$  because of  $\eta > -D$  and  $(1/D - 1/d_c) < 0$  because of  $d_c < D$ , the value of  $\beta$  is less than 1. Therefore, the exponent  $\beta$  presented by Eq. (30c) can take a value in the interval  $0 < \beta < 1$ . Finally, for Eq. (30d),  $\eta$  can be positive or negative. If  $\eta \geq 0$ , obviously  $\beta \geq 1$ , whereas  $0 < \beta < 1$  for  $-D < \eta < 0$ .

We can draw the phase diagram of our model from the above results. Figure 1(a) shows the regions of three distinct scaling behaviors in the parameter space of  $\eta$  and  $D$  under fixed values of  $m$  and  $\alpha$ , and Fig. 1(b) demonstrates those in the parameter space of  $\eta$  and  $m$  under fixed values of  $D$  and  $\alpha$ . The phase boundaries in Fig. 1(b) are translated from Fig. 1(a) by using Eq. (8). These results clearly show that superlinear scaling appears if  $\eta$  is positive and sublinear scaling if  $\eta$  is negative. Since the urban indicators  $Y(N)$  constructed by positive and negative  $\eta$  correspond to a creative productivity and infrastructure, respectively, these analytical results are consistent with urban scaling observed in the real world [15]. Note that we have linear scaling ( $\beta = 1$ ) on the phase boundaries. Thus, the condition  $\eta = 0$  always gives linear scaling regardless of the values of other parameters. This is reasonable because  $Y(N)$  for  $\eta = 0$  is nothing but the number of edges  $M$  in the network and  $M$  is proportional to  $N$  when  $\langle k \rangle$  is independent of  $N$ . The urban indicator that scales linearly corresponds

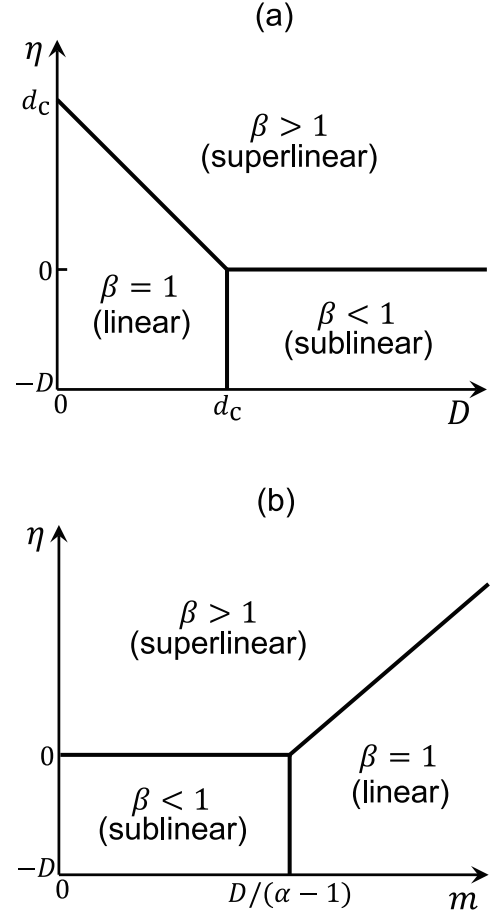


FIG. 1. Phase diagrams of our model (a) in the  $D$ - $\eta$  space with fixed values of  $m$  and  $\alpha$  and (b) in the  $m$ - $\eta$  space with fixed values of  $D$  and  $\alpha$ . On the phase boundaries represented by thick lines,  $\beta$  is equal to 1 (linear scaling).

to individual human needs such as the total number of houses.

It is found from Fig. 1(b) that  $Y(N)$  always obeys linear scaling for large enough  $m$ , i.e.,  $\beta = 1$  when the geographical constraint in the network formation is very strong. Since the network formed by a large  $m$  value has a lattice-like structure as mentioned below Eq. (8), lengths of edges in the network are almost constant. This is also

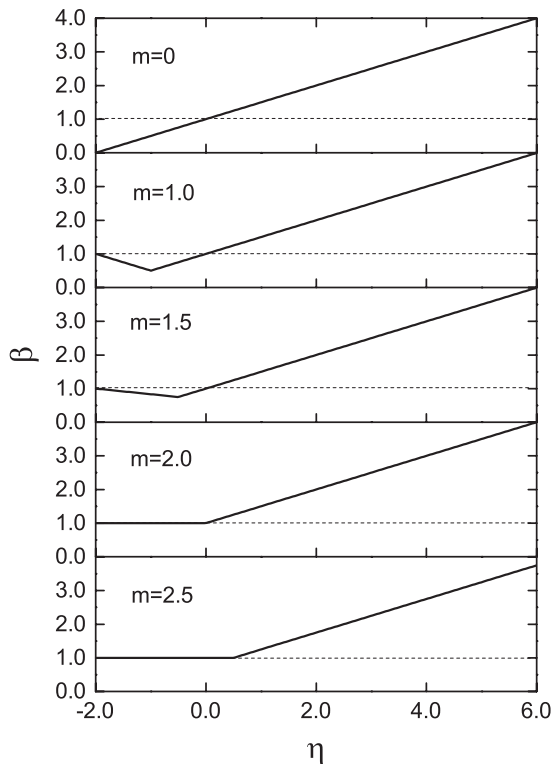


FIG. 2. Urban scaling exponent  $\beta$  as a function of  $\eta$  for several values of  $m$ . The exponents  $\alpha$  and the fractal dimension  $D$  are fixed at  $\alpha = 2.0$  and  $D = 2.0$ . Horizontal dashed lines at  $\beta = 1$  are guides to the eye, which separate the superlinear scaling region from the sublinear one.

confirmed by the fact that the edge-length distribution  $R(l)$  given by Eq. (9) becomes narrower as  $m$  increases. If edge lengths are constant, individual node-pair activities given by  $y_{ij} \propto l_{ij}^\eta$  are also constant. Denoting this constant by  $y_0$ , Eq. (18) provides  $Y(N) = N\langle k \rangle y_0 / 2$ , which leads to linear scaling.

#### IV. SIMULATION RESULTS

The urban scaling exponent  $\beta$  predicted by our model depends on the parameters  $D$ ,  $\alpha$ ,  $m$ , and  $\eta$ . Typical profiles of  $\beta$  given by Eq. (30) are presented in Figs. 2 and 3. Figure 2 shows the  $\eta$  dependence of  $\beta$  for various values of  $m$  under  $D = 2.0$  and  $\alpha = 2.0$ . It is verified that superlinear scaling of  $Y(N)$  requires  $\eta > 0$  and sublinear scaling is allowed only for  $\eta < 0$ . For any combination of  $m$ ,  $\alpha$ , and  $D$ , the exponent  $\beta$  linearly increases with  $\eta$  if  $\eta$  is large enough. The  $m$  dependence of  $\beta$  is depicted in Fig. 3(a) for various values of  $\eta$ . This figure clearly demonstrates that the urban indicator scales linearly with the population size if  $m$  is large enough, as pointed out in the previous section. The fact of  $\beta \neq 1$  at  $m = 0$  shows that the geographical constraint in the network formation is not necessary for nonlinear urban scaling, which does not

mean, however, that networks are not required to be embedded in the Euclidean space for obtaining nonlinear scaling of  $Y(N)$ . The exponent  $\beta$  changes with the fractal dimension  $D$  as shown in Fig. 3(b). In contrast to the  $m$  dependence,  $\beta$  depends non-monotonically on  $D$ . Although only results for  $\eta < d_c$  are shown here,  $\beta$  for  $\eta > d_c$  monotonically decreases with  $D$  and diverges at  $D = 0$ . Despite the lack of a physical meaning of the divergent  $\beta$  in the limit of  $D = 0$ , a large value of  $\beta$  at small  $D$  is reasonable because the system must have very long edges to keep  $\langle k \rangle$  constant and  $Y(N)$  increases rapidly with  $N$ .

Since the exponent  $\gamma$  characterizing the scale-free property of the network depends on  $d_c$  and  $D$  as presented by Eq. (7), it seems interesting to elucidate how the urban scaling exponent  $\beta$  varies with  $\gamma$ . The model parameter  $d_c$  giving  $\gamma = 2$  for a fixed  $D$  is, however, not uniquely determined if  $D \geq d_c$  [see the inset of Fig. 3(c)]. Thus,  $\beta$  for sublinear scaling that requires  $D \geq d_c$  cannot be related to  $\gamma$ . On the other hand, there is a one-to-one correspondence between  $\gamma$  and  $d_c$  for a fixed  $D$  if  $D < d_c$  that leads to superlinear or linear scaling. In this case, from Eqs. (30a) and (30b), the exponent  $\beta$  is expressed as

$$\beta = \begin{cases} 3 + \frac{\eta}{D} - \gamma & \text{if } 2 < \gamma < 2 + \frac{\eta}{D}, \\ 1 & \text{if } \gamma \geq 2 + \frac{\eta}{D}, \end{cases} \quad (31)$$

where  $\eta$  must be positive. The  $\gamma$  dependence of  $\beta$  for  $\eta > 0$  and  $\gamma > 2$  is illustrated in Fig. 3(c). From this argument, we can conclude that sublinear scaling is realized in a network with  $\gamma = 2$  and superlinear scaling appears for  $2 < \gamma < 2 + \eta/D$  in our model.

Let us confirm the above analytical results by numerical simulations. For simplicity, we treat the case of  $D = 2$ , namely,  $N$  nodes are uniformly distributed at random in a two-dimensional square space. The linear size  $L$  of the square space is adjusted to keep the node density constant with a change in  $N$ . The attractiveness  $x_i$  is assigned to each node according to the distribution function Eq. (3) with  $\alpha = 2.0$  and  $x_{\min} = 1.0$ . The Euclidean distance  $l_{ij}$  between nodes  $i$  and  $j$  is measured under periodic boundary conditions, and the threshold value  $\Theta$  in Eq. (5) is chosen so that the average degree becomes  $\langle k \rangle = 10.0$ . Networks formed by these conditions possess the scale-free property characterized by  $\gamma = 2$  for  $m \leq 2$  and  $\gamma = 1 + m/2$  for  $m > 2$ . The urban indicator  $Y(N)$  is calculated directly from the definition Eq. (18). Figure 4 shows the  $N$  dependence of  $Y(N)$  for various combinations of  $\eta$  and  $m$  in a double logarithmic scale. The longitudinal axis represents  $Y(N)/N$  rescaled by its value at the minimum  $N (= 1,000)$  to improve the legibility of the results. Thus, an increasing, decreasing, or constant straight line indicates superlinear, sublinear, or linear scaling of  $Y(N)$ , respectively. Our numerical results clearly show that  $Y(N)$  obeys a power law with respect to  $N$  and the slopes representing  $\beta - 1$  agree with the theoretical predictions indicated by dashed lines. Tri-

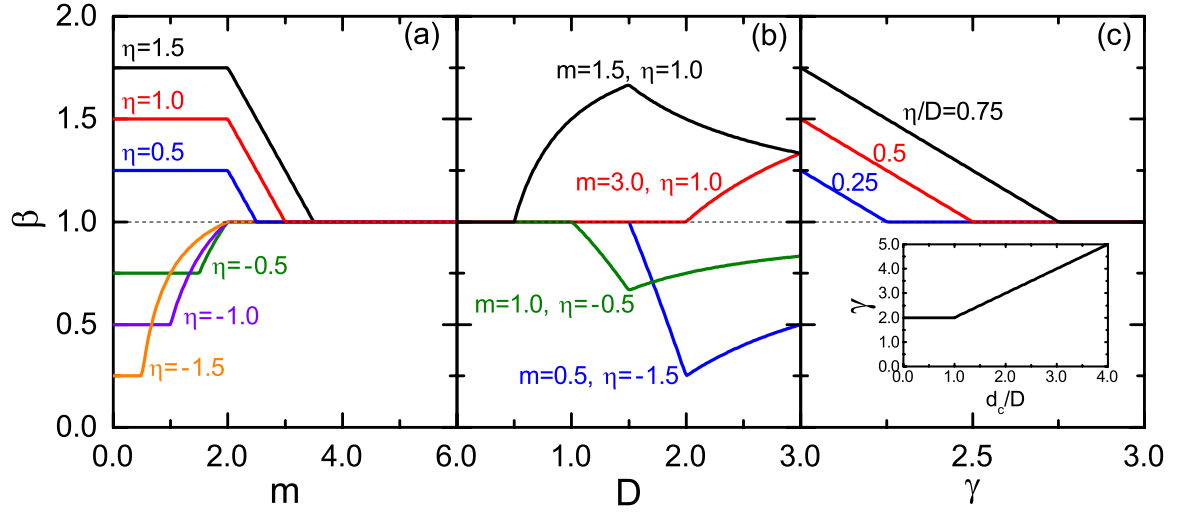


FIG. 3. (Color online) Profiles of the urban scaling exponent  $\beta$  as a function of  $m$ ,  $D$ , and  $\gamma$ . (a)  $\beta$  versus  $m$  for various values of  $\eta$ . The exponents  $\alpha$  and  $D$  are fixed as  $\alpha = 2.0$  and  $D = 2.0$ . (b)  $\beta$  versus  $D$  for various combinations of  $m$  and  $\eta$ . The exponent  $\alpha$  is fixed at  $\alpha = 2.0$ . (c)  $\beta$  versus  $\gamma$  for various positive values of  $\eta/D$ . Dashed line at  $\beta = 1$  in each panel separates the superlinear scaling region from the sublinear one. The inset of (c) shows the  $d_c/D$  dependence of the exponent  $\gamma$  given by Eq. (7).

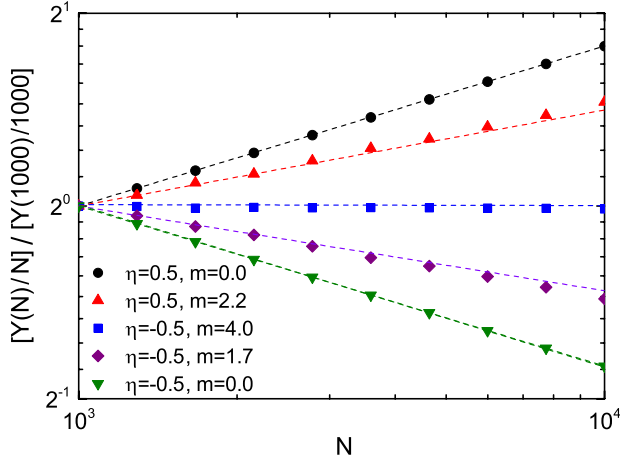


FIG. 4. (Color online) Numerically calculated urban indicators as a function of the population size (number of nodes)  $N$ . Nodes in geographical networks are scattered uniformly at random in two-dimensional square spaces ( $D = 2$ ) with a fixed node density. The exponent  $\alpha$  and the parameter  $x_{\min}$  characterizing the attractiveness distribution given by Eq. (3) are chosen as  $\alpha = 2.0$  and  $x_{\min} = 1.0$ . The longitudinal axis indicates  $Y(N)/N$  rescaled by its value at  $N = 1,000$ . Each symbol represents the result averaged over 1,000 realizations. Standard errors are smaller than the size of symbols. Circles, triangles, squares, diamonds, and inverted triangles are the results for  $(\eta = 0.5, m = 0)$ ,  $(\eta = 0.5, m = 2.2)$ ,  $(\eta = -0.5, m = 4.0)$ ,  $(\eta = -0.5, m = 1.7)$ , and  $(\eta = -0.5, m = 0)$ , respectively. Dashed lines through symbols from the top to the bottom give the theoretically predicted slopes of  $\beta - 1 = 0.25, 0.155, 0.0, -0.132, \text{ and } -0.25$ , respectively.

angles ( $\eta = 0.5$  and  $m = 2.2$ ) and diamonds ( $\eta = -0.5$  and  $m = 1.7$ ) in Fig. 4 slightly deviate from the corresponding theoretical lines. These deviations are caused by the finite-size effect as discussed below.

Next, we numerically calculated values of  $\beta$  as a function of  $m$  and compare the obtained results with the theoretical predictions. The exponent  $\beta$  is estimated by the least squares fit for numerical data of  $Y(N)$  within the range of  $10^3 \leq N \leq 10^4$ . Results for  $\eta = 0.5$  and  $\eta = -0.5$  are presented by filled circles and squares in Fig. 5, respectively. Parameters other than  $\eta$  and  $m$  and the computational conditions, such as the boundary conditions and the number of realizations for the sample average, are the same as those for Fig. 4. Standard errors over samples are less than the symbol size. Solid lines in Fig. 5 represent the theoretical predictions given by Eq. (30) for  $\eta = 0.5$  and  $-0.5$ . Numerical results roughly coincide with the theoretical curves. Especially, data for  $m > 4$  and  $m < 1$  agree quite well with the theoretical curves. However, simulation results near  $m = D/(\alpha - 1)$  and  $(D + \eta)/(\alpha - 1)$  that give the turnoff points of  $\beta(m)$  (i.e.,  $m = 2.0$  and  $2.5$  for  $\eta = 0.5$  and  $m = 2.0$  and  $1.5$  for  $\eta = -0.5$ ) deviate from the theoretical values. This is due to the finite-size effect. In the analytical calculation of the exponent  $\beta$ , we assume a large enough number of nodes to determine the dominant terms of Eqs. (14), (24), and (27). If two exponents of  $N$  in each of these equations becomes close to each other (i.e., approaching to the turnoff point), both terms almost equally contribute to  $Y(N)$  [or to  $\langle k \rangle$  for Eq. (14)], and  $Y(N)$  for numerically accessible  $N$  does not obey a power law any more. In order to demonstrate that the deviation of numerically calculated  $\beta$  near the turnoff point is caused by the



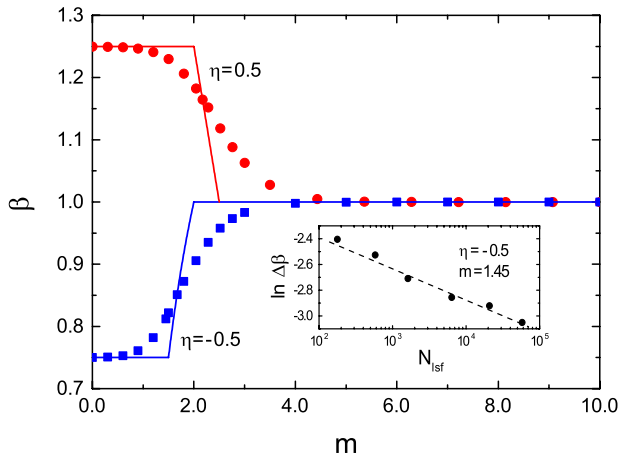


FIG. 5. (Color online) Numerically calculated  $m$  dependence of the exponent  $\beta$ . Circles and squares represent the results for  $\eta = 0.5$  and  $-0.5$ , respectively. All the conditions other than  $m$  and  $\eta$  are the same with those for Fig. 4. Solid lines give the theoretical predictions by Eq. (30) for  $\eta = 0.5$  and  $-0.5$  ( $\alpha = 2.0$  and  $D = 2.0$  for both lines). The inset shows the deviation  $\Delta\beta$  of  $\beta$  calculated numerically for  $\eta = -0.5$  and  $m = 1.45$  from its theoretical value as a function of  $N_{\text{lsf}}$  around which the least squares fit is performed within a narrow window of  $N$ . Dashed line in the inset is a guide to the eye.

finite-size effect, we show the network-size dependence of the deviation  $\Delta\beta$  of numerical data from the theoretical one in the inset of Fig. 5. For obtaining this inset, we calculated numerically  $Y(N)$  for  $\eta = -0.5$  and  $m = 1.45$  within the range of  $10^3 \leq N \leq 10^5$  and estimated  $\beta$  by the least squares fit for these data in relatively narrow windows of  $N$  around  $N_{\text{lsf}}$ . The result in the inset displays that the deviation  $\Delta\beta$  decreases with increasing  $N_{\text{lsf}}$ , which suggests  $\Delta\beta = 0$  in the thermodynamic limit ( $N \rightarrow \infty$ ).

## V. CONCLUSION

The origin of superlinear and sublinear scaling observed in urban indicators has been analytically argued by modeling the interrelationship of people in a city by a geographical scale-free network. In this network model, nodes close to each other are more likely to be connected than long distant nodes. We assumed that the urban indicator  $Y$  of a city is given by the sum of individual node-pair activities  $\{y_{ij}\}$  produced by personal, one-to-one human relationships in the city and  $y_{ij}$  is proportional to  $l_{ij}^\eta$ , where  $l_{ij}$  is the Euclidean distance between directly connected nodes  $i$  and  $j$ . For a positive or negative exponent  $\eta$ , the urban indicator represents a creative productivity or a degree of infrastructure development, respectively. We showed that the urban indicator obeys a power law  $Y(N) \propto N^\beta$  for a large enough population size  $N$ . The exponent  $\beta$  is larger than or equal to one

if  $\eta > 0$ , while  $0 < \beta \leq 1$  for  $\eta < 0$ , which implies that  $Y(N)$  corresponding to a creative productivity scales superlinearly or linearly with respect to the population size  $N$  and it scales sublinearly or linearly if  $Y(N)$  is a quantity related to infrastructure. This result coincides with the scaling behavior of real-world urban indicators. It has been also found that  $Y(N)$  is proportional to  $N$  if networks are formed under a strong geographical constraint. These results have been confirmed by numerical simulations.

In our argument, nodes are assumed to be placed on a  $D$  dimensional Euclidean space and the geographical distance plays a crucial role to understand urban scaling. To interpret  $Y(N)$  under a negative  $\eta$  as a degree of infrastructure development, the nodes must be arranged in a physical (geographic) space. This condition, however, can be relaxed for superlinear scaling. We can derive the same result for superlinear scaling of  $Y(N)$  even in the case that nodes are placed on a more general metric space in which Eqs. (5) and (17) with the abstract distance  $l_{ij}$  are a reasonable condition for the network formation and a plausible relation for the individual activity, respectively. For example, in a sociometric space, where social distances between nodes are defined, we can consider that nodes socially close to each other are more likely to be connected and a socially more distant node pair yields a higher productivity. Therefore, the scaling exponent  $\beta$  is also presented by Eq. (30) for  $\eta > 0$ , if Eqs. (5) and (17) with the social distance  $l_{ij}$  do actually hold. We should note that in such a case  $D$  must be the (fractal) dimension of the sociometric space.

We concentrated, in this work, on the average scaling behavior of the urban indicator. However, the actual urban indicators of individual cities deviate from the average values of  $Y(N)$  expected from their population sizes. Statistical properties of the fluctuations of  $Y(N)$  have been extensively studied by recent works [18–21]. Within the framework of the present model, we can also consider such fluctuations by evaluating  $Y(N)$  defined by Eq. (16) instead of its average given by Eq. (18). The fluctuations in the urban indicators of cities with the same population size  $N$  are caused, in our model, by different network configurations due to different spatial arrangements of nodes and different assignments of the attractiveness. In addition to this structural network effect, the deviation of  $Y(N)$  from the average value could arise from the fluctuations in the model parameters. There are four parameters in our model, i.e.,  $m$  characterizing the strength of the geographical constraint in the network formation,  $\alpha$  describing how widely distributed the attractiveness is, the fractal dimension  $D$  of the population density, and  $\eta$  specifying the Euclidean-distance dependence of the individual activity. Although this work assumes that these four parameters remain constant over a set of cities, violation of this assumption will also lead to fluctuations in the urban indicator. By comparing statistical properties of the predicted fluctuations of  $Y(N)$  to those observed in actual urban indicators we would be able to assess how



well our model describes urban scaling phenomena.

## ACKNOWLEDGMENTS

This work was supported by a Grant-in-Aid for Scientific Research (No. 22560058) from Japan Society for the Promotion of Science, by the project SEETechnology “Co-operation of SEE science parks for the promotion of transnational market uptake of R&D results and technologies by SMEs” co-funded by South East Europe Transnational Cooperation Programme, and by the oper-

ation entitled “Centre for Open Innovation and Research of the University of Maribor”. The last operation is co-funded by the European Regional Development Fund and conducted within the framework of the Operational Programme for Strengthening Regional Development Potentials for the period 2007–2013, development priority 1: “Competitiveness of companies and research excellence”, priority axis 1.1: “Encouraging competitive potential of enterprises and research excellence”.

Numerical calculations in this work were performed in part on the facilities of the Supercomputer Center, Institute for Solid State Physics, University of Tokyo.

- 
- [1] M. Rubner, *Zeit. Biol.* **19**, 535 (1883).
  - [2] M. Kleiber, *Hilgardia* **6**, 315 (1932).
  - [3] S. Nordbeck, *Geogr. Anal. B* **53**, 54 (1971).
  - [4] M. Batty and P. A. Longley, *Fractal Cities: A Geometry of Form and Function*, (Academic Press, London, 1994).
  - [5] M. Batty, *Science* **319**, 769 (2008).
  - [6] M. Batty, R. Carvalho, A. Hudson-Smith, R. Milton, D. Smith, and P. Steadman, *Eur. Phys. J. B* **63**, 303 (2008).
  - [7] M. Batty, *Cities* **29**, S9 (2012).
  - [8] C. P. Lo, *Ann. Assoc. Am. Geogr.* **92**, 225 (2002).
  - [9] D. Pumain, Santa Fe Institute, Working Paper 2004-02-002.
  - [10] H. Samaniego and M. E. Moses, *J. Transp. Land Use* **1**, 21 (2008).
  - [11] Y. Chen and S. Jiang, *Chaos Soliton. Fract.* **39**, 49 (2009).
  - [12] Y. Chen, *Discrete Dyn. Nat. Soc.* **2010**, 22 (2010).
  - [13] E. L. Glaeser and B. Sacerdote, *J. Polit. Econ.* **107**, S225 (1999).
  - [14] C. Kühnert, D. Helbing, and G. West, *Physica A* **363**, 96 (2006).
  - [15] L. M. A. Bettencourt, J. Lobo, D. Helbing, C. Kühnert, and G. B. West, *Proc. Natl. Acad. Sci. USA* **104**, 7301 (2007).
  - [16] L. M. A. Bettencourt, J. Lobo, and D. Strumsky, *Res. Policy* **36**, 107 (2007).
  - [17] L. M. A. Bettencourt, J. Lobo, and G. B. West, *Eur. Phys. J. B* **63**, 285 (2008).
  - [18] L. M. A. Bettencourt, J. Lobo, D. Strumsky, and G. B. West, *PLoS ONE* **5**, e13541 (2010).
  - [19] A. Gomez-Lievano, H. Youn, and L. M. A. Bettencourt, *PLoS ONE* **7**, e40393 (2012).
  - [20] L. G. A. Alves, H. V. Ribeiro, E. K. Lenzi, and R. S. Mendes, *PLoS ONE* **8**, e69580 (2013).
  - [21] J. Lobo, L. M. A. Bettencourt, D. Strumsky, and G. B. West, *PLoS ONE* **8**, e58407 (2013).
  - [22] L. M. A. Bettencourt, J. Lobo, and H. Youn, arXiv:soc-ph/1301.5919v.
  - [23] M. A. Changizi and M. Destefano, *Complexity* **15**, 11 (2010).
  - [24] S. Arbesman and N. A. Christakis, *Physica A* **390**, 2155 (2011).
  - [25] L. Wu and J. Zhang, *Phys. Rev. E* **84**, 026113 (2011).
  - [26] L. G. A. Alves, H. V. Ribeiro, and R. S. Mendes, *Physica A* **392**, 2672 (2013).
  - [27] M. Fragkias, J. Lobo, D. Strumsky, and K. C. Seto, *PLoS ONE* **8**, e64727 (2013).
  - [28] W. Pan, G. Ghoshal, C. Krumme, M. Cebrian, and A. Pentland, *Nat. Commun.* **4**, 1961 (2013).
  - [29] L. N. Lamsal, R. V. Martin, D. D. Parrish, and N. A. Krotkov, *Environ. Sci. Technol.* **47**, 7855 (2013).
  - [30] S. Arbesman, J. M. Kleinberg, and S. H. Strogatz, *Phys. Rev. E* **79**, 016115 (2009).
  - [31] L. M. A. Bettencourt, *Science* **340**, 1438 (2013).
  - [32] R. J. Smeed, *J. Inst. Highw. Eng.* **10**, 5 (1963).
  - [33] P. Frankhauser, *Population: an English selection* **10**, 205 (1998).
  - [34] S.-H. Yook, H. Jeong, and A.-L. Barabási, *Proc. Natl. Acad. Sci. USA* **99**, 13382 (2002).
  - [35] Y. Chen, *Int. J. Urban Sustain. Dev.* **1**, 89 (2010).
  - [36] N. Masuda, H. Miwa, and N. Konno, *Phys. Rev. E* **71**, 036108 (2005).
  - [37] K. Yakubo and D. Korošak, *Phys. Rev. E* **83**, 066111 (2011).
  - [38] D. Liben-Nowell, J. Nowak, R. Kumar, P. Raghavan, and A. Tomkins, *Proc. Natl. Acad. Sci. USA* **102**, 11623 (2005).
  - [39] L. Adamic and E. Adar, *How to search a social network*, *Soc. Netw.* **27**, 187 (2005).
  - [40] J. Goldenberg and M. Levy, arXiv:soc-ph/0906.3202.
  - [41] R. Lambiotte, V. D. Blondel, C. de Kerchove, E. Huens, C. Prieur, Z. Smoreda, and P. Van dooren, *Physica A* **387**, 5317 (2008).